Received: 24 February 2019 | Accepted: 9 October 2019

DOI: 10.1002/stem.3112

Authored by a member of

IFATS International Federation for Adipose Therapeutics and Science

STEM CELLS

TISSUE-SPECIFIC STEM CELLS

CD10 expression identifies a subset of human perivascular progenitor cells with high proliferation and calcification potentials

Lijun Ding[1,2,3] | Bianca Vezzani[2,4] | Nusrat Khan[2] | Jing Su[1] | Lu Xu[1] | Guijun Yan[1] | Yong Liu[5] | Ruotian Li[6] | Anushri Gaur[2] | Zhenyu Diao[1] | Yali Hu[1] | Zhongzhou Yang[7] | W. Reef Hardy[8] | Aaron W. James[8,9] | Haixiang Sun[1,10] | Bruno Péault[2,8]

[1]Center for Reproductive Medicine, Department of Obstetrics and Gynecology, The Affiliated Drum Tower Hospital of Nanjing University Medical School, Nanjing, People's Republic of China

[2]MRC Center for Regenerative Medicine and Center for Cardiovascular Science, University of Edinburgh, Scotland, UK

[3]Clinical Center for Stem Cell Research, The Affiliated Drum Tower Hospital of Nanjing University Medical School, Nanjing, People's Republic of China

[4]Department of Morphology, Surgery and Experimental Medicine, Section of General Pathology, University of Ferrara, Ferrara, Italy

[5]Department of Experimental Medicine, The Affiliated Drum Tower Hospital of Nanjing University Medical School, Nanjing, People's Republic of China

[6]Department of Cardiology, The Affiliated Drum Tower Hospital of Nanjing University Medical School, Nanjing, People's Republic of China

[7]State Key Laboratory of Pharmaceutical Biotechnology and MOE Key Laboratory of Model Animal for Disease Study, Model Animal Research Center, Nanjing Biomedical Research Institute, Nanjing University, Nanjing, People's Republic of China

[8]Orthopedic Hospital Research Center and Broad Stem Cell Center, David Geffen School of Medicine, University of California, Los Angeles, California

[9]Department of Pathology, Johns Hopkins University, Baltimore, Massachusetts

[10]Key Laboratory of Pharmaceutical Biotechnology, Nanjing University, Nanjing, People's Republic of China

Correspondence
Haixiang Sun, PhD, Center for Reproductive Medicine, Department of Obstetrics and Gynecology, The Affiliated Drum Tower Hospital of Nanjing University Medical School, 321 Zhongshan Road, Nanjing 210008, People's Republic of China.
Email: stevensunz@163.com

Bruno Péault, PhD, Orthopedic Hospital Research Center and Broad Stem Cell Center, David Geffen School of Medicine, University of California at Los Angeles, 615 Charles E. Young Drive South, Room 546, Los Angeles, CA 90095.
Email: bpeault@mednet.ucla.edu

Funding information
Musculoskeletal Transplant Foundation; Maryland Stem Cell Research Foundation; American Cancer Society, Grant/Award Number: RSG-18-027-01-CSM; Department of Defense, Grant/Award Numbers: W81XWH-18-10613, W81XWH-18-1-0336, W81XWH-18-1-0121; NIH/NIAMS, Grant/Award Numbers: R21 DE027922, K08 AR068316, R01 AR070773; BIRAX Regenerative Medicine Initiative; British Heart

Abstract

The *tunica adventitia* ensheathes arteries and veins and contains presumptive mesenchymal stem cells (MSCs) involved in vascular remodeling. We show here that a subset of human adventitial cells express the CD10/CALLA cell surface metalloprotease. Both $CD10^+$ and $CD10^-$ adventitial cells displayed phenotypic features of MSCs when expanded in culture. However, $CD10^+$ adventitial cells exhibited higher proliferation, clonogenic and osteogenic potentials in comparison to their $CD10^-$ counterparts. $CD10^+$ adventitial cells increased expression of the cell cycle protein CCND2 via ERK1/2 signaling and osteoblastogenic gene expression via NF-κB signaling. CD10 expression was upregulated in adventitial cells through sonic hedgehog-mediated GLI1 signaling. These results suggest that CD10, which marks rapidly dividing cells in other normal and malignant cell lineages, plays a role in perivascular MSC function and cell fate specification. These findings also point to a role for $CD10^+$ perivascular cells in vascular remodeling and calcification.

Foundation; Jiangsu Province Social Development Project, Grant/Award Number: BE2018602; Nanjing Medical Science Development Project, Grant/Award Number: ZKX16042; Nature Science Foundation of China, Grant/Award Numbers: 81600353, 81571391, 81871128; National Key Research and Development Program of China, Grant/Award Number: 2018YFC1004700

KEYWORDS

adventitia, CD10, GLI1, osteogenesis, mesenchymal stem cell, SHH, vascular calcification

1 | INTRODUCTION

Mesenchymal stem/progenitor cells (MSCs) have been derived in cultures from many human tissues, including bone marrow, fat, skeletal muscle, endometrium, placenta, umbilical cord, and deciduous teeth.[1-7] Notwithstanding their anatomic origin, cultured MSCs display the same fibroblast-like morphology, are multipotent and immunosuppressive,[8,9] allowing for multiple therapeutic applications.[10] Perivascular cells are now commonly accepted as innate ancestors of MSCs.[11-16] Both adventitial cells constituting the outmost layer of large arteries and veins, and pericytes surrounding capillaries and microvessels express MSC markers in situ and give rise to bona fide MSCs in culture.[16,17] Single-cell transcriptomes have revealed a hierarchical organization of perivascular adventitial cells and pericytes, the former being the most developmentally primitive.[18] In agreement, adventitial cells can be precursor cells for pericytes.[17-19]

Both pericytes and adventitial cells participate in the regeneration and turnover of the mouse dental pulp, where the neurovascular bundle (NVB) has been identified as a niche where sonic hedgehog (SHH) secreted by NVB sensory nerves regulates mesenchymal progenitor cell homeostasis.[19] GLI1 is the only transcription factor whose expression is induced by SHH signaling.[20,21] SHH/GLI1 signaling has been proven to maintain the MSC pool and GLI1+ adventitial cells act as pro-fibrotic progenitors in mouse organs.[20,21]

CD10, also known as common acute lymphoblastic leukemia antigen (CALLA), membrane metallo-endopeptidase (MME), and neutral endopeptidase, is a zinc-dependent metalloprotease that cleaves peptides at the amino side of hydrophobic residues. CD10/CALLA has been mostly studied, as early as the 1970s, as a marker of lymphoid progenitors, acute lymphocytic leukemias, and other hematologic malignancies.[22] It was more recently realized that CD10 is also expressed in epithelial tumors.[23]

We report herein that CD10 is natively coexpressed on subsets of pericytes and adventitial cells in human tissues. FACS sorted CD10-expressing adventitial cells show higher expression of cell cycle G1/S specific cyclin D2 (CCND2) and neural EGFL like 1 (NELL1), and exhibit higher proliferation and osteoblastic differentiation in culture than $CD10^-$ adventitial cells. CD10 expression was upregulated in $CD10^+$ adventitial cells by SHH/GLI1 signaling, which in turn sustained high expression of CCND2 and NELL1. These results suggest CD10 as a novel marker of osteogenic perivascular presumptive MSCs in human tissues.

Significance statement

Perivascular adventitial cells include multipotent progenitor cells giving rise in culture to mesenchymal stem/progenitor cells. The present data show that a subset of human adventitial cells natively express the CD10 surface marker, regulated by sonic hedgehog/GLI1 signaling. Purified $CD10^+$ adventitial cells exhibit high proliferative, clonogenic and osteogenic potentials, suggesting a role in pathologic vascular remodeling.

2 | MATERIALS AND METHODS

2.1 | Human tissues

Human fetal tissues were obtained from spontaneous or voluntary pregnancy interruptions at Edinburgh Royal Infirmary (University of Edinburgh, UK) or Nanjing Drum Tower Hospital (Nanjing University Medical School, China), with the approval of institutional review boards (No. SZ2013-002) and consent of patients. Abdominal subcutaneous white adipose tissues (WAT) and lipoaspirates were obtained with review board approval from consenting patients (aged from 27 to 55 years) undergoing abdominoplasty at the Murrayfield clinic (Edinburgh, UK) and Department of Burns and Plastic Surgery (Nanjing Drum Tower Hospital, Nanjing, China). Calcified arterial segments from peripheral arterial disease (PAD) patients were obtained from consenting donors (ages from 58 to 86 years) undergoing vascular surgery at Nanjing Drum Tower Hospital.

2.2 | Immunohistochemistry

Fresh tissues were embedded in OCT (Leica, Wetzlar, Germany) and frozen in liquid nitrogen. WAT was first immersed in gelatin/sucrose, then embedded in OCT and frozen in liquid nitrogen. Sections (5-12 μm thick) were serially cut on a cryostat (Leica) and fixed for 5 minutes with either acetone and methanol solution (1:1, vol:vol) or 4% paraformaldehyde (PFA). Sections were permeabilized using PBS/0.1% Triton X-100 solution for 5 minutes at room temperature (RT) and blocked with protein-blocker (DPB-125, Spring Bioscience, UK) for half an hour. Primary antibodies were incubated overnight at 4°C.

After washing with PBS, sections were incubated for 1 hour at RT with species-specific secondary antibodies. All antibodies were diluted

in antibody dilution medium (Invitrogen, Carlsbad, California). Antibodies and dilutions used are listed in Table S1. Non-immune immunoglobulins of the same isotypes were used as controls with each immunostaining. Biotinylated *Ulex europaeus* agglutinin 1 (UEA-1, 1:100, Vector B1065, Vector Laboratories, Burlingame, California) incubated 1.5 hours at RT and then Alexa Fluor 488 conjugated to streptavidin (1:200, Invitrogen, S11223, Life Technologies, Carlsbad, California) incubated for half an hour, which was used to detect human endothelial cells. Nuclei were stained with 4′,6-diamidino-2-phenylindole (DAPI) (Invitrogen). Sections were mounted with fluoromount-G (Southern Biotech, Birmingham, Alabama) and observed on a fluorescence microscope (Zeiss Observer, Zeiss, Oberkochen, Germany; Olympus BX61, Olympus, Tokyo, Japan).

CD10 expression was analyzed in paraffin embedded calcified arterial segments from 15 PAD patients (Rutherford categories 4-6) and in control normal arterial edges. Antibodies and dilutions used are listed in Table S1. Images were processed using Fiji software[24] or ZEN Blue lite version (Zeiss).

Cells (at passage 2) were fixed for 10 minutes with 4% PFA, permeabilized with PBS/0.1% Triton X-100 and blocked with protein-blocker (DPB-125) for 30 minutes at RT. Antibodies and dilutions used are also listed in Table S1. All primary antibodies were diluted in antibody diluent (Life Technologies) and incubated at 4°C overnight. FITC- or PE-conjugated secondary antibodies were used for the analysis. A non-immune immunoglobulin of the same isotype was used as a control with each immunostaining. After nuclei staining with DAPI, cells were observed as above. Images were processed using Fiji software.[24]

2.3 | Flow cytometry

Tissues (fetal muscle, kidney, heart, liver, and placenta) were cut into small pieces in DMEM (Gibco, Fisher Scientific, New York) containing 1% penicillin/streptomycin (PS), 1% fetal calf serum (FCS) (Gibco), and collagenases I, II, and IV (all at the final concentration of 1 mg/mL, Gibco), then incubated at 37°C for 1 hour in a shaking water bath (180 rpm). Fetal long bones were cut into halves and bone marrow was flushed out using the same medium as above, and then processed identically. Digestion was performed using collagenases I, II, and IV (final concentration of 0.5 mg/mL, Gibco), then incubated at 37°C for 30 minutes in a shaking water bath. Adult WAT was minced and digested in DMEM containing 1% BSA (Sigma, St Louis, Missouri) and collagenase II (1 mg/mL, Gibco) for 45 minutes in a shaking water bath (180 rpm) at 37°C.

All the samples were then washed with 2% FCS/PBS (Sigma Aldrich) and filtered sequentially through 100- and 70-μm cell strainers (BD Falcon, Corning, New York). After centrifugation, pellets were resuspended in erythrocyte lysis buffer (155 mM NH_4Cl, 170 mM Tris, pH 7.65, all from Sigma-Aldrich) for 15 minutes at RT. Cells were washed again with 2% FCS/PBS and filtered through 40-μm cell strainers (BD Falcon) to obtain single cell suspensions.

Cells from all above human tissues were then used for multicolor immunofluorescence staining as previous described.[25] Cells in suspension (10^5 for analysis and above 5×10^7 for sorting) were incubated with a combination of the following conjugated mouse anti-human antibodies (1:100, all from Becton-Dickinson, San Diego, California): anti-CD45-APC cy7 (557833), anti-CD56-PE cy7 (557747), anti-CD144-percp cy5.5 (561566), anti-CD34-PE (555822), anti-CD146-FITC (560846), and anti-CD10-APC (340923) diluted in 2% FCS/PBS at 4°C for 15 minutes in the dark. Analysis was performed on a BD LSR Fortessa 5-laser flow cytometer (BD Biosciences) using Diva software (v.6.0, BD Biosciences). Sorting was performed on an FACS Aria II cell sorter (BD Biosciences). Single stained beads were used as compensation controls. Data were analyzed using FlowJo (v.10.0, FlowJo, Ashland, Oregon). Forward scatter area (FSC-A) versus side scatter area (SSC-A) gate was used to identify cells, followed by FSC-A versus forward scatter height (FSC-H) to select single cells. Viable cells were gated as negative for DAPI staining. Sorted cells were plated at a density of $2 \times 10^4/cm^2$ in 0.2% gelatin-coated plates and cultured at 37°C in EGM2 medium (Lonza, Basel, Switzerland) for 2 weeks. Attached cells were maintained in culture in basal medium consisting of DMEM Glutamax (Gibco) supplemented with 100 μg/mL streptomycin (Sigma-Aldrich), 100 U/mL penicillin (Sigma-Aldrich) and 20% heat-inactivated FCS (Gibco). Cells were used before passage 5 (p5).

Cultured cells from WAT at passage 2 were stained with directly labeled antibodies (Table S2). Cells were then washed twice and at least 5×10^4 events were acquired on a CantoII cytometer (BD Biosciences).

2.4 | Cell proliferation assay

A Cell Counting Kit-8 (CCK-8, Dojindo Molecular Technologies, Rockville, Maryland) was used for detection of cell proliferation according to manufacturer's instructions. Briefly, 10 μL CCK-8 solution was added to each well and incubated for 3 hours. Absorbance at 450 nm, directly proportional to the number of living cells, was measured on a microplate reader (Thermo Electron, Waltham, Massachusetts).

2.5 | Colony-forming unit assay

$CD10^+$ and $CD10^-$ adventitial cells were seeded at densities of 10, 50, and 100 cells/cm^2, and incubated at 37°C, 5% CO_2 for 2 weeks. Cells were fixed with 4% PFA for 10 minutes at RT then stained with 0.1% crystal violet. Colonies were counted under the microscope after five washes with 10% acetic acid.

2.6 | Cell cloning

Cultured $CD10^+$ and $CD10^-$ adventitial cells from the same WAT sample were sorted by FACS into a 96-well plate at a density of 1 cell/well. After 4 weeks, clones reached confluence. Four individual clones obtained from each WAT sample (n = 3) were randomly selected and subpassaged into new 96-well plates at a density of 1 cell/well. Colony formation potential was assessed.[17]

2.7 | In vitro mesodermal differentiation potential

For osteogenic differentiation, $CD10^+$ and $CD10^-$ adventitial cells at 70% confluence were cultivated in STEMPRO osteogenic differentiation medium (Gibco). After 28 days, cells were fixed in 4% PFA for 2 minutes and incubated for 10 minutes with alizarin red (pH 4.2) or von Kossa reagent for detection of calcium deposits.

For chondrogenesis, high-density pellets were prepared by spinning down 5×10^5 cultured cells in 15 mL conical tubes and grown in STEMPRO chondrogenic differentiation medium (Gibco) for 21 days. Pellets were fixed in 10% formalin, dehydrated using a graded series of ethanol washes, and embedded in paraffin. Five-micrometer thick sections were rehydrated and stained with alcian blue and nuclear fast red for detection of sulfated glycosaminoglycans and nuclei, respectively.

For adipogenic differentiation, $CD10^+$ and $CD10^-$ adventitial cells at 70% confluence were cultured in STEMPRO adipogenic differentiation medium (Gibco) for 14 days. Cells were fixed in 2% PFA at RT, washed in 60% isopropanol, and incubated with oil red O for 10 minutes at RT for detection of lipids.

All mesodermal differentiation assays were performed in technical triplicates, and cells cultured in basal medium were used as negative controls.

2.8 | Microarray analysis

Total RNA was isolated using TRIzol (Invitrogen) and treated with DNaseI (Promega, Madison, Wisconsin) to remove any contaminating genomic DNA. RNA quality was evaluated using spectrophotometry and denaturing agarose gel electrophoresis. Genome-wide gene expression patterns of WAT-derived $CD10^+$ and $CD10^-$ cultured adventitial cells at primary passage were assessed using human OneArray Plus gene microarrays (HOA6.2, Phalanx Biotech, Taiwan, China). Gene expression was analyzed by Genechem (Shanghai, China). Differentially expressed genes were identified using LIMMA[26] in *R* using a twofold cutoff and a false discovery rate <0.05. Heatmaps were generated using Genesis.[27] Boxplots were generated in *R*, the middle line representing the median, the box showing the 25th and 75th percentile, and the whiskers extending to Q1-1.5 × IQR/Q3 + 1.5 × IQR. GO and KEGG pathways were analyzed with the Cluster 3.0 software.

2.9 | Quantitative real-time PCR

cDNA was synthesized from 1 μg of purified total RNA using a PrimeScript RT reagent kit (Bio-Rad Laboratories, Hercules, California), according to the manufacturer's instructions. The primers used for quantitative PCR analysis are listed in Table S3. Each real-time PCR reaction were performed on a LightCycler 480 system (Roche, Basel, Switzerland): 95°C 3 minutes; 94°C 10 seconds, 60°C 30 seconds, 72°C 30 seconds, 40 cycles. Each sample was analyzed in triplicate, and the experiment was performed three times. Relative transcript abundance was determined according to the Pfaffl's $2^{-\triangle\triangle C(T)}$ method, and the fold change in expression of each gene was normalized to an endogenous control (18S rRNA).

2.10 | Western blotting

WAT-derived $CD10^+$ and $CD10^-$ adventitial cells (2×10^4 cells/cm^2) were seeded onto 10-cm cell culture dishes. Cells were incubated with MEK selective inhibitor PD98059 (50 μM, #9900, Cell Signaling Technologies, Danvers, Massachusetts), NF-κB inhibitor pyrrolidine dithiocarbamate (PDTC) (25 μM, ab141406, Abcam) or GLI1 inhibitor GANT61 (10 μM, HY-13901, Medchem Express, Shanghai, China) for 24 or 48 hours. After the treatment, the cells were rinsed twice with precooled PBS, after which 1 mL of cell lysis buffer (50.0 mM Tris pH = 7.6, 150.0 mM NaCl, 0.1% sodium dodecyl sulfate (SDS), 1.0% NP-40, protease inhibitor cocktail) was added, and the cells were scraped off. Cells were lysed at 4°C for 30 minutes under rotation, centrifuged at 15,000 rpm for 30 minutes, and the supernatant was collected. Protein concentrations were determined by the BCA Protein Assay Reagent (Thermo Fisher Scientific). 20 μg of total proteins were loaded on 10% SDS-polyacrylamide electrophoresis gel and then transferred to a polyvinylidene fluoride membrane. The membrane was treated with 5% nonfat milk in TRIS-buffered saline and Tween 20 for 1 hour at RT. Primary antibody was incubated overnight at 4°C (antibodies listed in Table S4). Secondary species-specific antibodies conjugated to horseradish peroxidase were added for 1 hour at RT. Immunoreactive bands were detected using ECL Western Blotting Detection Reagent.

2.11 | Knockdown of CD10 in adventitial cells

To evaluate CD10 contribution to the proliferation and osteogenic differentiation of adventitial cells, CD10 expression was downregulated using a siRNA. SiRNAs for CD10 (si-CD10-1: CAACCTACGATGATGGTAT; si-CD10-2: GGATGGATGCCGAGACAAA; si-CD10-3: GGCCAGAG TATGCGGTTAA, Ribobio, Guangzhou, China) were transfected into $CD10^+$ adventitial cells by using Lipofectamine 3000 Reagent (Invitrogen) according to manufacturer's instructions. A scrambled, control siRNA (si-NC) was used as a negative control for si-CD10 (Ribobio). Briefly, 50 nM of siRNA and 3 μL of Lipofectamine 3000 Reagent were diluted in 100 μL of serum- and antibiotics-free DMEM. The resultant mixture was gently blended. The siRNA diluent was slowly added dropwise to the lipid diluent and thoroughly mixed before incubation at RT for 15 minutes. Next, the mixture was seeded onto cells cultured in a 24-well plate and incubated at 37°C, 5% CO_2 for 48 hours.

2.12 | Gene expression induction by growth factors

Expression of CD10 in cultured $CD10^+$ and $CD10^-$ adventitial cells was assessed in the presence of growth factors (bFGF, BDNF, EGF, GDNF, HGF, LIF, SHH, TGFβ1, and VEGF). Growth factor dilutions

and combinations are specified in Table S5. Gene expression was measured by qRT-PCR at 24 hours after the addition of SHH protein (100 ng/mL) in cultured $CD10^+$ and $CD10^-$ adventitial cells. Protein expression (*CD10*, *PTCH1*, *GLI1*, *GLI2*, *CCND2*, *NELL1*, and *GAPDH*) in cultured $CD10^+$ and $CD10^-$ adventitial cells was detected by Western blotting analysis at 48 hours after the addition of SHH protein (100 ng/mL).

2.13 | Statistical analysis

All data were analyzed using SPSS 18.0 software. Quantitative data are presented as mean ± standard deviation. Comparisons between the means of two groups were made using the Student's *t*-test or Mann-Whitney *U* test. Statistical analysis was performed by One-way analysis of variance with the Student-Newman-Keuls test for experiments involving more than two groups. *P* values less than .05 were considered statistically significant.

3 | RESULTS

3.1 | CD10 expression in the human perivascular compartment

Pericytes (CD34−CD146+), which encircle capillaries and microvessels, and adventitial cells (CD34+CD146−) that reside in the *tunica adventitia* of larger arteries and veins represent a perivascular source of MSCs.[16,17] Since CD10 has been described at the surface of a subset of MSC-like cells,[28-32] we assessed the expression of this metalloproteinase by perivascular presumptive MSCs. Immunohistochemistry was performed on five adult WAT samples, where CD10 was found expressed mainly in perivascular areas (Figure 1). CD10 is present on a subset of pericytes, which also express αSMA and NG2 (Figure 1A,B). Perivascular CD10 expressing cells do not express the hematopoietic cell marker CD45 (Figure 1C). A subgroup of adventitial cells, typified by CD34 expression, also express CD10 (Figure 1D,E). Except for pericytes and adventitial cells, perivascular smooth muscle cells also express CD10, albeit at different extents (Figure 1D,E).

3.2 | $CD10^+$ adventitial cells are present in multiple human organs

To confirm and quantify the expression of CD10 in adventitial cells, multicolor FACS analysis was performed on sixteen WAT samples (27-55 years), 12 placentas (18 weeks to term), 9 fetal long bone marrows (FBM) (12-22 weeks), 8 fetal hearts (17-23 weeks), 8 fetal skeletal muscles (17-23 weeks), 8 fetal livers (17-23 weeks), and 8 fetal kidneys (17-23 weeks). Dead cells ($DAPI^+$), then $CD45^+$ hematopoietic cells and $CD56^+$ myogenic cells were gated out. CD144 was used to negatively select endothelial cells (Figure 2A-D). Adventitial cells were identified and selected by high CD34 expression and absence of CD146, which also ensures the removal of pericytes.[16,17,33] $CD10^+$ and $CD10^-$ subsets of adventitial cells were then identified. $CD45^-CD56^-CD144^-CD146^-CD34^+CD10^+$ adventitial cells were detected in WAT, placenta, FBM, and fetal muscle (Figure 2E-I). Conversely, no or very few adventitial cells expressed CD10 in fetal kidney, heart, and liver (Figure 2J-L). Percentages of $CD10^+$ cells in total adventitial cells varied between organs, averaging 52.52% (37.9%-70.3%) in WAT, 51.5% (20.1%-72.4%) in placenta, 67.1% (56.8%-77.4%) in FBM, and 38.77% (21.2%-60.6%) in fetal muscle (Table S6).

3.3 | Sorted $CD10^+$ and $CD10^-$ adventitial cells behave differently in culture

$CD10^+$ and $CD10^-$ adventitial cells were sorted from 16 WATs, 12 placentas (18 weeks to term), 9 FBMs (14-22 weeks) and seeded in culture (Figure 3A). $CD10^+$ adventitial cells adhered to culture dishes within 24 hours, exhibiting spindle-like morphology. $CD10^-$ adventitial cells adhered more slowly, displaying an elongated shape (Figure 3B). As shown by cell proliferation analysis (Figure 3C,D), $CD10^+$ adventitial cells divided faster than their $CD10^-$ counterparts.

Perivascular stem cells, that is, adventitial cells and pericytes, are tissue-resident presumptive MSCs and possess colony-forming unit (CFU)-f potential.[16,17] When seeded at 10, 50, and 100 cells/cm^2, $CD10^+$ adventitial cells sorted from WAT and placenta had a higher CFU-f content than $CD10^-$ adventitial cells ($P < .01$) (Figure 3E, Figure S1). Sorted $CD10^+$ and $CD10^-$ WAT-derived adventitial cells were seeded clonally in 96-well plates. Cloning efficiency was much higher in the $CD10^+$ adventitial cell population than in the $CD10^-$ counterpart (20.8% ± 3.80% vs 2.76% ± 1.95%, $P < .01$) (Figure 3F). After culture, four clones derived from each adventitial cell subset (n = 3) were chosen arbitrarily and tested for subcloning potential in vitro. WAT $CD10^+$ cell derived clones still displayed 11.3% cloning efficiency, whereas clonal growth ability was lost from $CD10^-$ cell derived clones (Figure 3G).

WAT-derived total adventitial cells can be readily cultured into MSCs, exhibiting multilineage differentiation capacity toward osteocytes, chondrocytes, and adipocytes.[17,34] Surface markers were analyzed by flow cytometry on WAT-derived $CD10^+$ and $CD10^-$ cultured adventitial cells at passage 2. Neither cell subset expressed CD14, CD31, CD45, CD56, CD117, CD146, CD271, KDR, or HLA-DR (Figure 3H, Figure S2). Conversely, both cultured $CD10^+$ and $CD10^-$ adventitial cells expressed CD9, CD13, CD29, CD73, CD90, and CD105 (Figure 3H, Figure S2). Three markers (CD10, CD34, and CD54) were differentially expressed by cultured $CD10^+$ and $CD10^-$ adventitial cells (Figure 3H). Expression of CD10 and CD34 was lost by approximately 23.3% ± 4.2% and 72% ± 7.0% of cultured $CD10^+$ adventitial cells, respectively. Of note, a minor subset of cultured $CD10^-$ adventitial cells appeared to express low levels of surface CD10 (Figure 3H), suggesting CD10 induction in vitro. For this reason, cultured $CD10^-$ adventitial cells should be qualified as being $CD10^{lo/-}$, although only the $CD10^-$ phenotype will be further mentioned for the

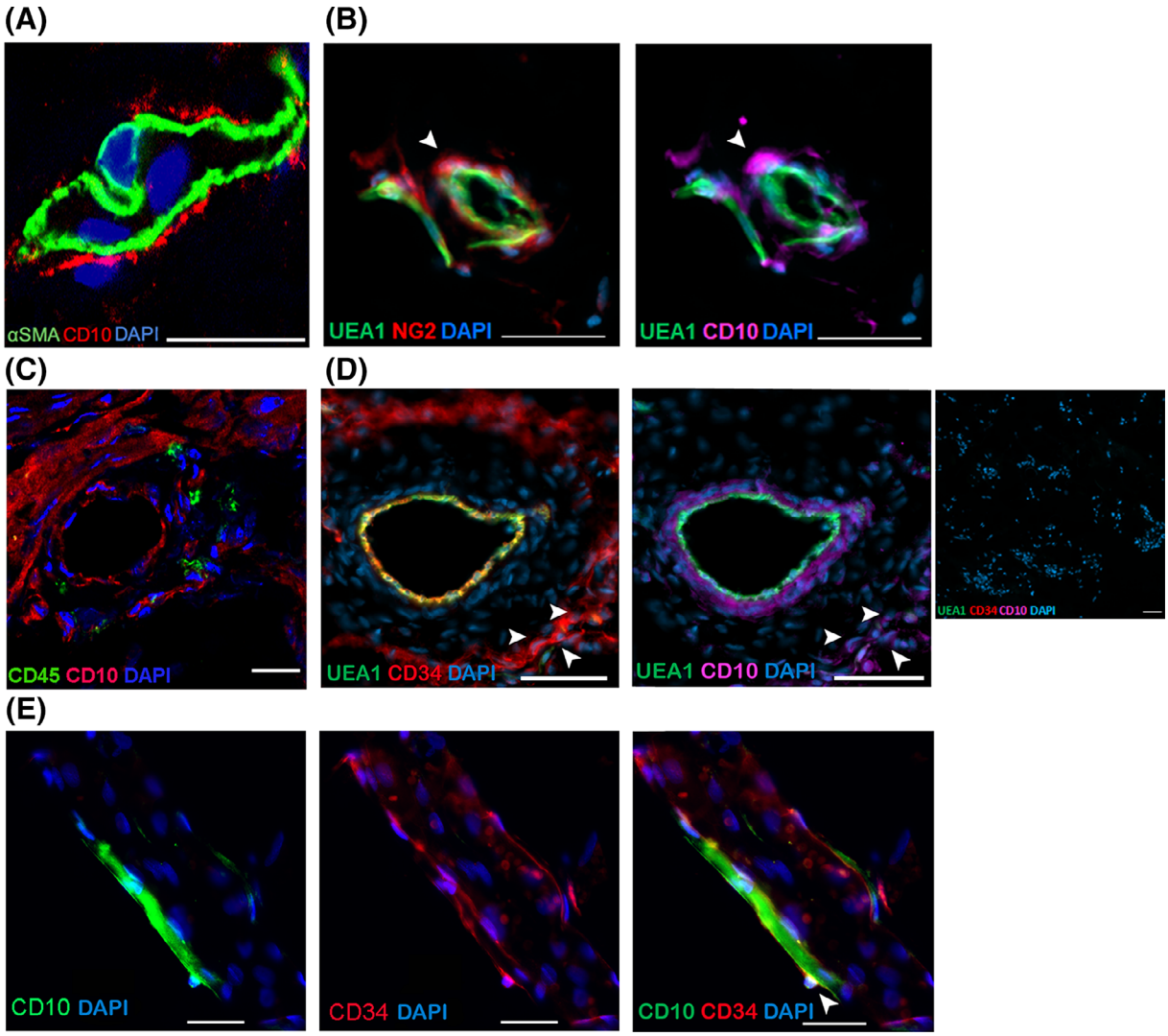

FIGURE 1 Immunohistochemical detection of CD10 and other vascular cell markers in human white adipose tissue (WAT). A, A CD10-positive pericyte (red) also expressing αSMA (green) encircles a capillary. Scale bar, 10 μm. B, Around microvessels, some pericytes marked by NG2 expression (red) also express CD10 (purple). Endothelial cells are marked by UEA-1 uptake (green) (white arrowheads). Scale bar, 50 μm. C, CD10-expressing perivascular cells (red) do not express the hematopoietic cell marker CD45 (green). Scale bar, 25 μm. D, In the arterial *adventitia*, CD34-positive cells (red) are concentric to UEA1-positive endothelial cells (green) (white arrowheads). Some of these $CD34^+$ adventitial cells co-express CD10 (purple) (white arrowheads). Scale bar, 20 μm. Negative control for UEA1, CD10, and CD34 antibody shows in small figure. Scale bar, 25 μm. E, CD10 (green) and CD34 (red) double-positive cells (white arrowheads) are seen on a transverse section of the adventitia. Scale bar, 50 μm

sake of simplicity. Surprisingly, 46.6% ± 3.1% cultured $CD10^+$ adventitial cells expressed CD54 (ICAM-1), which marks stage transition toward induced-pluripotent stem cells in vitro.[35] By contrast, cultured $CD10^-$ adventitial cells did not express CD34 nor CD54. Immunocytochemistry showed that both cultured $CD10^+$ and $CD10^-$ adventitial cells express CD44, and sporadically αSMA but did not demonstrate immunoreactivity for POU5F, NANOG, SOX9, NG2, nor PDGFRβ (Figure S3).

$CD10^+$ and $CD10^-$ adventitial cells sorted from WAT were next cultured until passage 3, and induced to differentiate toward mesodermal cell lineages (Figure 4A-D). $CD10^+$ adventitial cells cultured in osteogenic medium for 28 days yielded higher percentages of alkaline phosphatase (ALP)-positive cells (85% ± 6%) than the same number of $CD10^-$ adventitial cells cultured under the same conditions (34% ± 2%, $P < .05$) (Figure 4A,E). After culture in osteogenic medium, most $CD10^+$ adventitial cells were stainable with alizarin red S, displaying confluent bone nodules, compared with only patchy mineralization in the $CD10^-$ subset (Figure 4B,F). $CD10^+$ adventitial cells from placenta also showed higher capacity for osteogenic differentiation than $CD10^-$ adventitial cells, as assessed by ALP and von Kossa staining (Figure S4). Furthermore, osteogenesis associated genes (*RUNX2*, *BGLAP*, *and COL1A1*) were more expressed in $CD10^+$ adventitial cells compared with $CD10^-$ adventitial cells after cultured in osteogenic medium ($P < .05$) (Figure 4G).

After 28 days of induction, chondrogenic differentiation was detected in both subsets of adventitial cells, but pellets from $CD10^+$

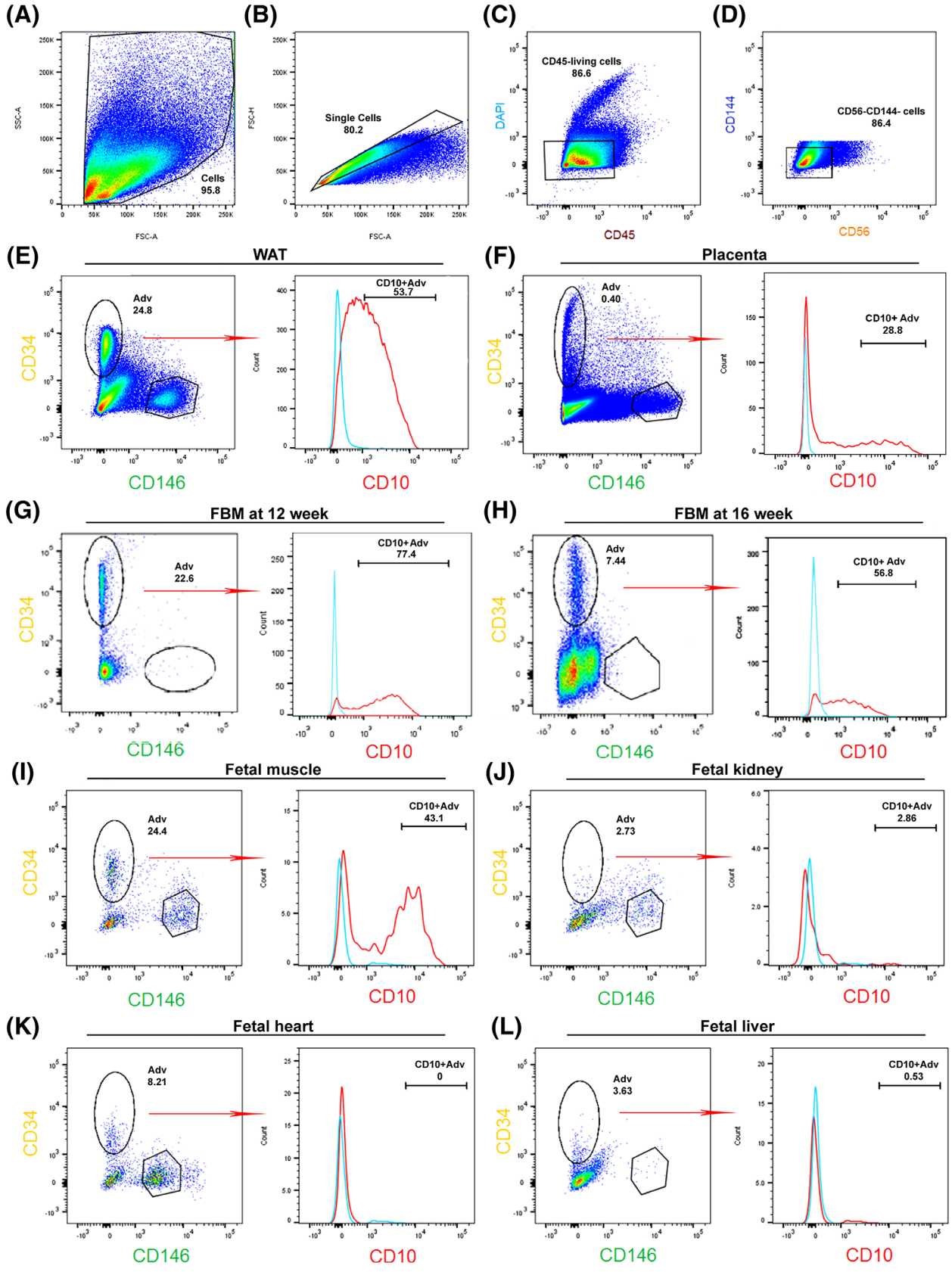

FIGURE 2 Flow cytometry analysis of CD10$^+$ adventitial cells in multiple human tissues. A-D, Tissues were dissociated with collagenase, and single-cell suspensions were stained with directly labeled antibodies and analyzed on an FACS Aria II cell sorter, following double scatter cell selection (A), single cell selection (B), exclusion of DAPI$^+$ dead cells and CD45$^+$ hematopoietic cells (C), CD56$^+$ muscle cells and CD144$^+$ endothelial cells (D). E-L, CD34$^+$CD146$^-$ adventitial cells were sorted and percentages of CD10$^+$ adventitial cells are shown for (E), adult white adipose tissue (n = 16); (F) placental villi (n = 12); (G) 12-week fetal bone marrow (n = 3); (H) 16-week fetal bone marrow (n = 3); (I) fetal skeletal muscle (n = 8); (J) fetal kidney (n = 8); (K) fetal heart (n = 8); (L) fetal liver (n = 8). See also Table S6. Adv, adventitial cells

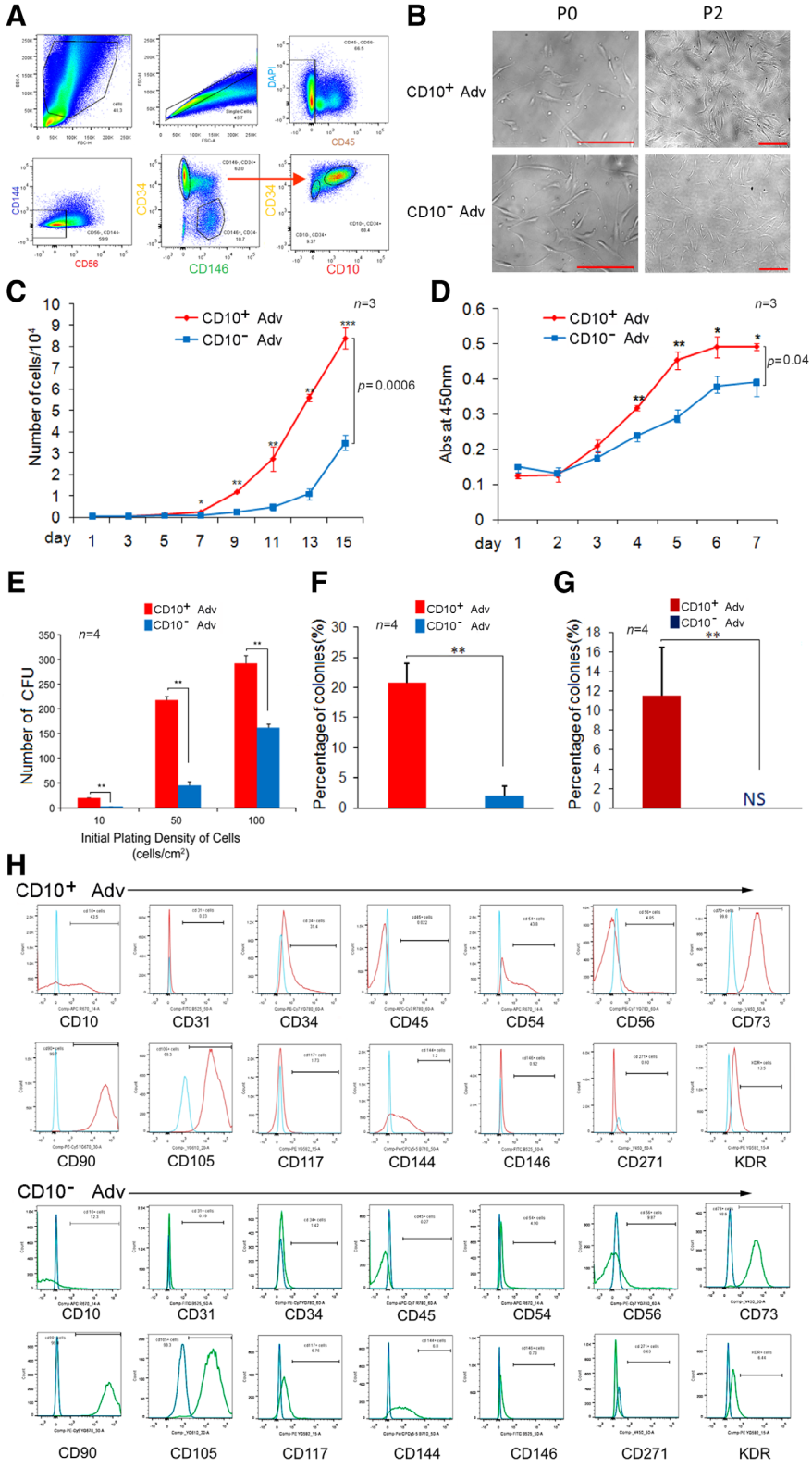

FIGURE 3 In vitro culture of WAT $CD10^+$ and $CD10^-$ adventitial cells. A, $CD10^+$ and $CD10^-$ adventitial cells were purified by FACS from adipose tissue. B, $CD10^+$ and $CD10^-$ adventitial cells show different morphologies in culture (scale bar, 50 μm). C, $CD10^+$ adventitial cells proliferate faster than $CD10^-$ counterparts at the cell density of 500 cells/cm^2 (mean ± SD, n = 3). D, CCK-8 analysis confirms that $CD10^+$ adventitial cells divide more quickly than $CD10^-$ adventitial cells (mean ± SD, n = 3). E, $CD10^+$ adventitial cells include more CFU-f than $CD10^-$ adventitial cells, as assessed at different plating cell densities (mean ± SD, n = 4). F, Clonogenic cells are more frequent among $CD10^+$ adventitial cells than $CD10^-$ counterparts (mean ± SD, n = 4). G, Clonogenic cell numbers remain higher in $CD10^+$ adventitial cell derived clones, after passage, than in $CD10^-$ adventitial cell derived clones (mean ± SD, n = 4). H, The immunophenotype of cultured $CD10^+$ and $CD10^-$ adventitial cells was analyzed by flow cytometry after labeling with antibodies to CD10, CD31, CD34, CD45, CD54, CD56, CD73, CD90, CD105, CD117, CD144, CD146, CD271, and KDR (n = 4). *P < .05; **P < .01; ***P < .001. All statistical analyzes used Student's t-test. See also Figures S1, S2, and S3. Adv, adventitial cells; CFU, colony-forming unit

adventitial cells were 3 ± 1.2 times larger than those from $CD10^-$ adventitial cells (Figure 4C). Culture of $CD10^+$ and $CD10^-$ adventitial cells in adipocyte differentiation medium led to the appearance of intracellular lipid droplets stainable by Oil Red O (Figure 4D). There was no obvious difference regarding adipocyte differentiation between these two cell subsets.

Since the presence of osteogenic cells in the walls of human blood vessels may be directly relevant to the etiology of arteriosclerosis, we assessed CD10 expression in calcified arterial segments from 15 patients with PAD. Atheriosclerotic occlusion and calcification were confirmed by HE staining (Figure 4H). CD10 expression was abundant in the calcified arterial adventitia, in comparison with normal artery controls (Figure 4H,I).

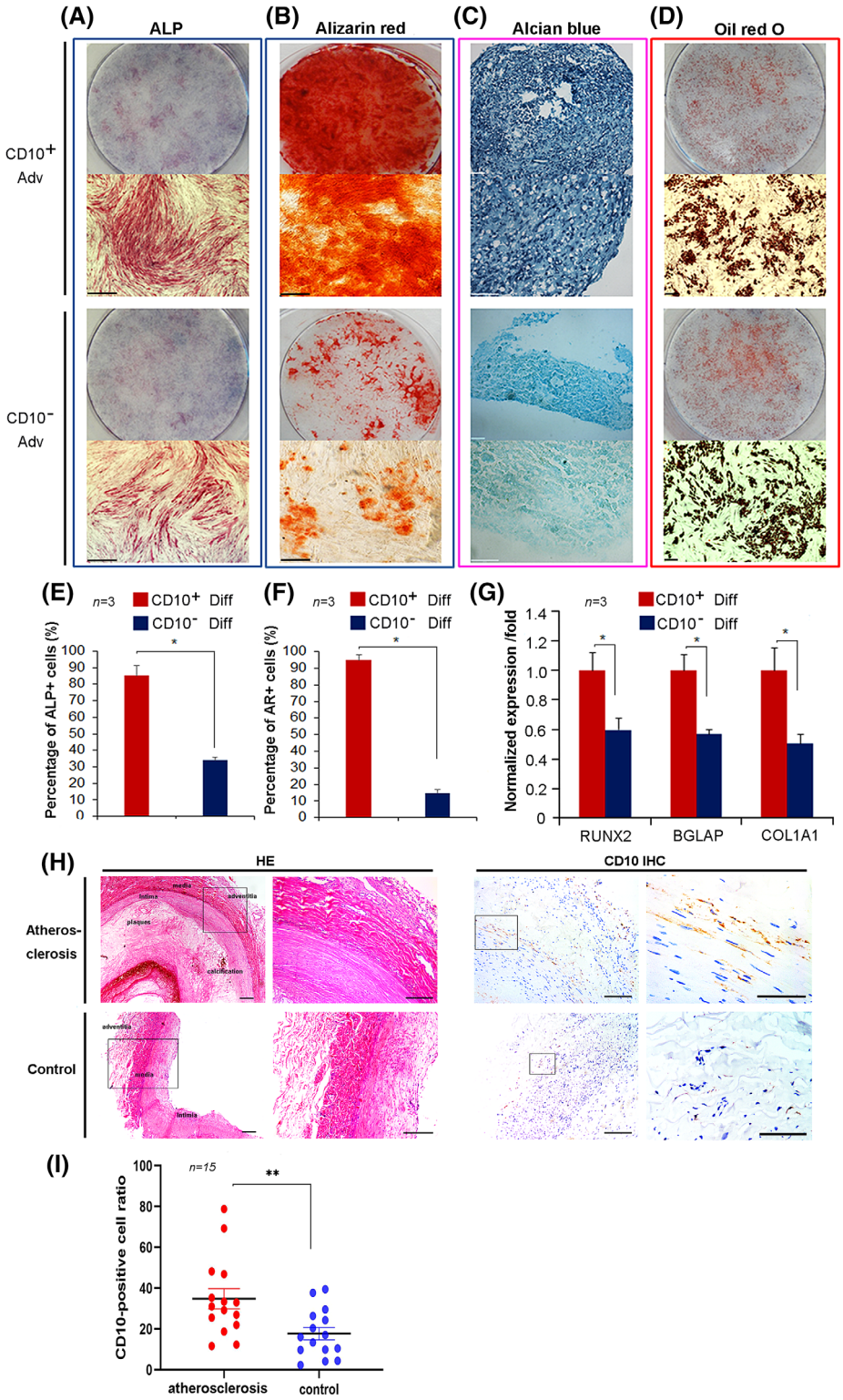

FIGURE 4 WAT CD10$^+$ and CD10$^-$ adventitial cell differentiation into mesodermal cell lineages. CD10$^+$ and CD10$^-$ adventitial cells differentiate into osteocytes, chondrocytes and adipocytes after induction. A and B, Alkaline phosphatase (ALP) staining and Alizarin red (AR) staining reveal osteocytes. Nuclei were stained with hematoxylin. Scale bars, 50 μm. C, Alcian blue staining shows chondrocytes. Scale bars, 50 μm. D, Oil red O staining indicates the presence of adipocytes. Scale bars, 50 μm. E, ALP-positive cells were counted among 500 randomly selected WAT-derived CD10$^+$ and CD10$^-$ adventitial cells after osteogenesis induction. F, AR-positive cells were counted among 500 randomly selected WAT-derived CD10$^+$ and CD10$^-$ adventitial cells after osteogenesis induction. G, Gene expression in WAT-derived CD10$^+$ and CD10$^-$ adventitial cells after osteogenesis induction. All experiments were performed three times. H, Hematoxylin-eosin and CD10 IHC staining of calcified arterial segments from peripheral arterial disease (PAD) patients and normal arterial controls. Scale bars, 50 μm. I, CD10-positive cell numbers in calcified arterial adventitias from 15 PAD patients, compared with healthy controls. *P < .05, **P < .01. All statistical analyzes used Student's t-test. See also Figure S4. Adv, adventitial cells

3.4 | Expression of genes related to self-renewal and osteogenesis differs between CD10$^+$ and CD10$^-$ adventitial cells

CD10$^+$ and CD10$^-$ adventitial cells sorted from WAT (n = 3) were cultured at 20,000 cells /cm^2 for 7 days. 5,000-50,000 cells were used to screen changes in genome-wide gene expression by microarray analysis. Among 31,000 genes, a total of 710 were differentially expressed (log2 [fold change] ≥ 1.0 and P < .05). Of note, 502 genes were more highly expressed in CD10$^+$ adventitial cells and 208 were upregulated in CD10$^-$ adventitial cells (Figure 5A). GO analysis (Figure 5B) revealed that CD10$^+$ adventitial cells preferentially expressed metalloproteinase genes including *CD10 (MME)* (Figure 5C), and genes regulating cell proliferation including *CCND2*

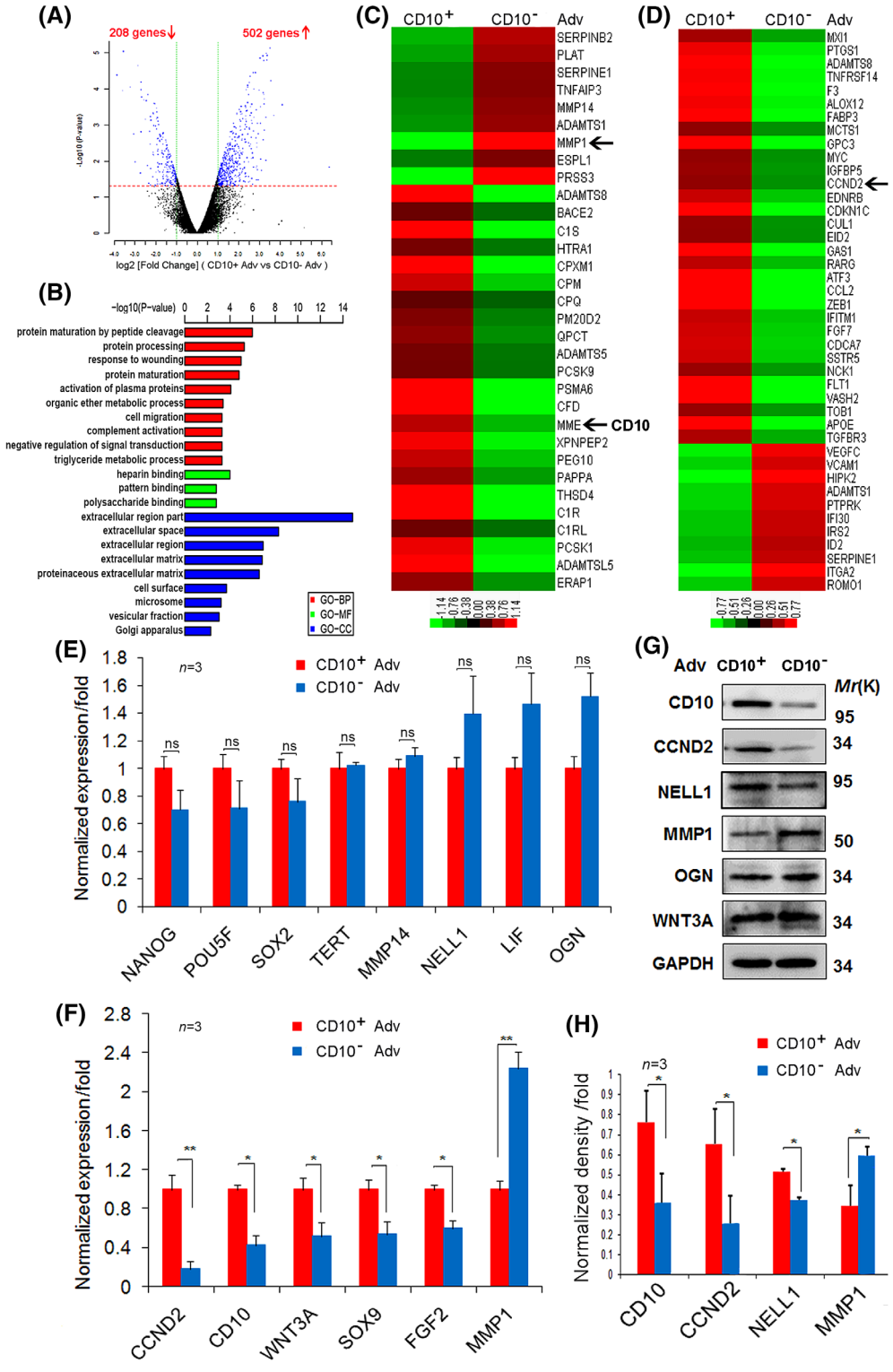

FIGURE 5 Gene expression in WAT CD10$^+$ and CD10$^-$ adventitial cells. A, Comparison of gene expression patterns using Human OneArray Plus (Phalanx). Five hundred two upregulated genes and 208 downregulated genes differ between the two cell subsets (twofold or greater). B, Go analysis illustrating genes differently expressed between CD10$^+$ and CD10$^-$ adventitial cells. C and D, Marked increase in expression of genes involved in metalloproteinase activity and cell proliferation in CD10$^+$ adventitial cells, compared with CD10$^-$ adventitial cells. E, Expression of "stemness" genes is not different between CD10$^+$ and CD10$^-$ adventitial cells (mean ± SD, n = 3). *P < .05; **P < .01. Pairwise one-tailed t-test. F, Expression of CD10, CCND2, and NELL1 is higher in CD10$^+$ adventitial cells (mean ± SD, n = 3). *P < .05; **P < .01. Pairwise one-tailed t-test. G, Western blot analysis shows that expression of CD10, CCND2, and NELL1 is increased, but that of MMP1 decreased in CD10$^+$ adventitial cells (n = 3). H, CD10, CCND2, NELL1, and MMP1 protein level was analyzed by band density scanning and calculation. *P < .05; **P < .01. Pairwise one-tailed t-test. See also Figure S5. Adv, adventitial cells

(Figure 5D). Distinctly expressed genes in CD10$^+$ and CD10$^-$ adventitial cells are involved in complement and coagulation cascades (11 genes; Figure S5A, B). qRT-PCR was used to detect the expression of genes of interest. *CCND2*, *CD10*, *WNT3A*, *SOX9*, *FGF2*, and *MMP1* were differentially expressed in CD10$^+$ and CD10$^-$ adventitial cells, but other "stemness" associated and other genes from the microarray were not (Figure 5E,F). Western blotting analysis further showed that higher levels of CD10, CCND2, and NELL1 are expressed in CD10$^+$ adventitial cells, whereas CD10$^-$ adventitial cells expressed higher levels of MMP1 (Figure 5G,H). Protein amounts of OGN and WNT3A were not significantly different (Figure 5G).

3.5 | Proliferation and bone formation by CD10$^+$ adventitial cells are decreased after CD10 knockdown

To explore the role of CD10 signaling in the self-renewal and osteogenic potential of WAT adventitial cells, different siRNAs were used to reduce the expression of CD10. Transfection into CD10$^+$ adventitial cells of these siRNAs, especially si-CD10-3, reduced CD10 mRNA to 31.85% of the amount observed after transfection with negative control siRNA (si-NC) (Figure 6A). CD10 protein was also decreased to approximately 25% of the si-NC control (Figure 6B). Concomitantly, mRNA levels of CCND2 and NELL1 were decreased to 52.60%, and 46.80%, respectively (Figure 6C). Western blotting analysis showed that CCND2 and NELL1 protein amounts were significantly decreased after downregulation of CD10 (Figure 6D), indicating that CD10 signaling directly affects the expression of CCND2 and NELL1.

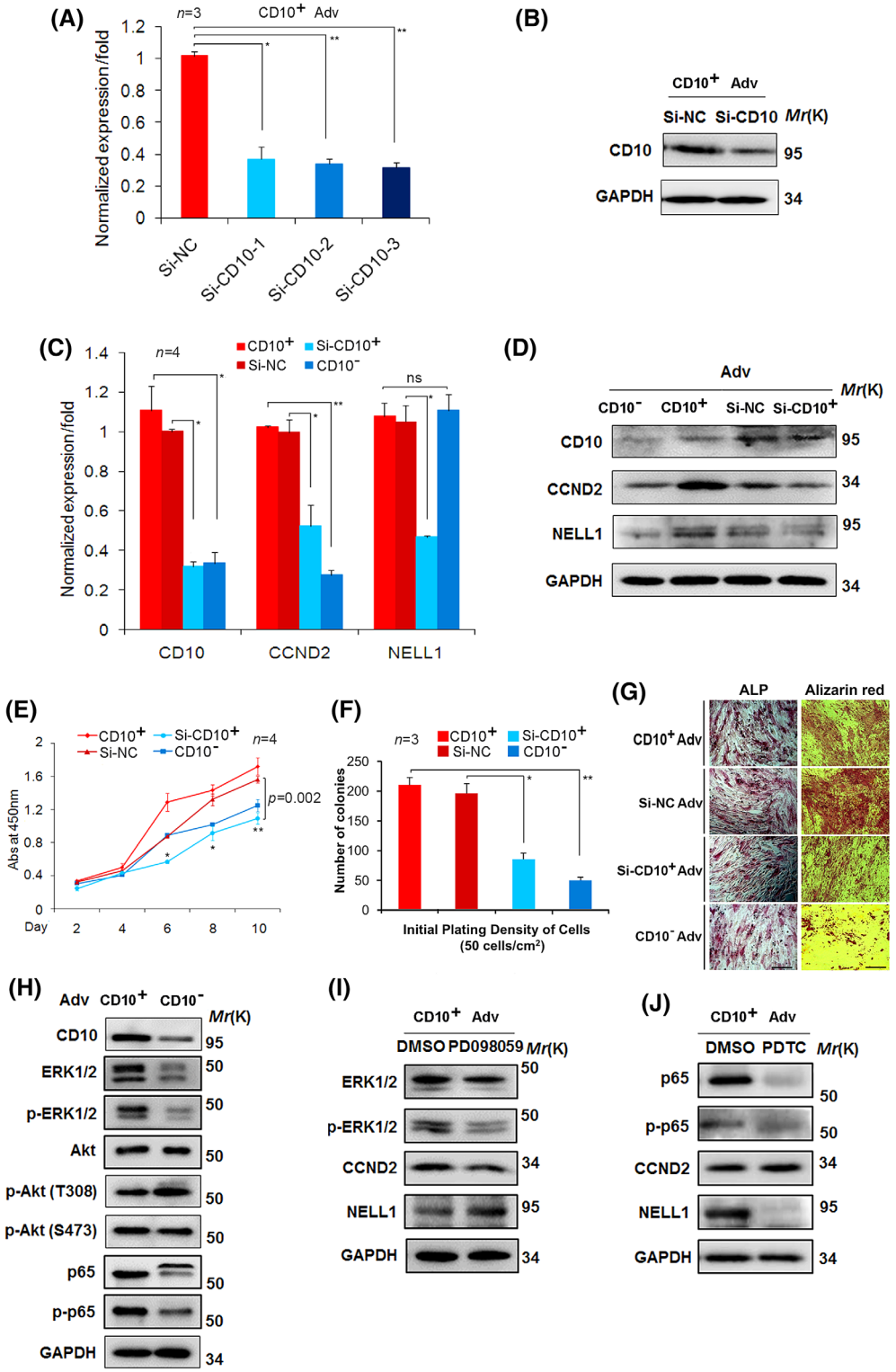

FIGURE 6 Knockdown of CD10 decreases CCND2 and NELL1 expression and affects WAT adventitial cell phenotype. A, CD10 expression detected by qRT-PCR after RNA interference using siRNAs (mean ± SD, n = 3). *P < .05; **P < .01. One-way analysis of variance (ANOVA) with the Student-Newman-Keuls test. B, Western blot detection of CD10 after siRNA interference (n = 3). C, Expression of CCND2 and NELL1 was detected by qRT-PCR after knockdown of CD10 (mean ± SD, n = 4). *P < .05; **P < .01. One-way ANOVA with the Student-Newman-Keuls test. D, Western blot detection of CCND2 and NELL1 after CD10 down-regulation (n = 3). E, CCK-8 analysis of CD10$^+$ and CD10$^-$ adventitial cell proliferation after knockdown of CD10 (mean ± SD, n = 4). *P < .05; **P < .01. One-way ANOVA with the Student-Newman-Keuls test. F, CFU-f in CD10$^+$ and CD10$^-$ adventitial cells after knockdown of CD10 (mean ± SD, n = 3). *P < .05; **P < .01. One-tailed t-test. G, ALP and Alizarin red staining of differentiated CD10$^+$ and CD10$^-$ adventitial cells after knockdown of CD10 expression (n = 3). Scale bars, 20 μm. H, Signaling molecules detected in CD10$^+$ and CD10$^-$ adventitial cells by Western blot analysis. ERK1/2 and NF-κB related molecules were analyzed in both subsets of adventitial cells (n = 3). I, The ERK1/2 inhibitor, PD098059, was used. CCND2 and NELL1 expression was detected (n = 3). J, The p65 inhibitor PDTC was used to inhibit NF-κB activity. CCND2 and NELL1 expressions were analyzed (n = 3). Adv, adventitial cells; CFU, colony-forming unit

In addition, proliferation of CD10$^+$ WAT adventitial cells slowed down after downregulation of CD10, compared with controls ($P < .01$) (Figure 6E), as the number of colonies produced in the CFU-f assay decreased ($P < .05$) (Figure 6F). Upon osteogenic differentiation, ALP- and alizarin red S-positive cells were significantly reduced in number in CD10$^+$ adventitial cells treated with CD10 siRNA (Figure 6G), reflecting a decrease in bone-forming ability.

CCND2 (cyclin D2) plays an important role in stem cell proliferation, and NELL1 controls osteogenesis.[36,37] A possible role of CD10 in the regulation of CCND2 and NELL1 expression, via relevant molecular pathways, was investigated in CD10$^+$ and CD10$^-$ WAT adventitial cells. Regarding PI3K-AKT, there were no significant differences in the expression of AKT, pAKT (T308) and pAKT (S473) in CD10$^+$ and CD10$^-$ adventitial cells (Figure 6H). As of MAPK, expression of ERK1/2 and pERK1/2 was higher in CD10$^+$ than in CD10$^-$ adventitial cells (Figure 6H). Additionally, along the NF-κB pathway, P65 and p-P65 levels were higher in CD10$^+$ adventitial cells than in CD10$^-$ counterparts (Figure 6H).

To assess the regulation of CCND2 expression, an MAPK inhibitor, PD098059, was used to block ERK1/2 activation. The expression of NELL1 was unchanged, but CCND2 expression decreased after PD098059 treatment of CD10$^+$ adventitial cells (Figure 6I). Furthermore, a selective NF-κB inhibitor, PDTC, was used to inhibit P65 and p-P65 expression in CD10$^+$ adventitial cells. NELL1 expression was then totally inhibited but CCND2 was not affected (Figure 6J). These results suggest that CD10 affects the expression of CCND2 via ERK1/2 and that of NELL1 via NF-κB in adventitial cells.

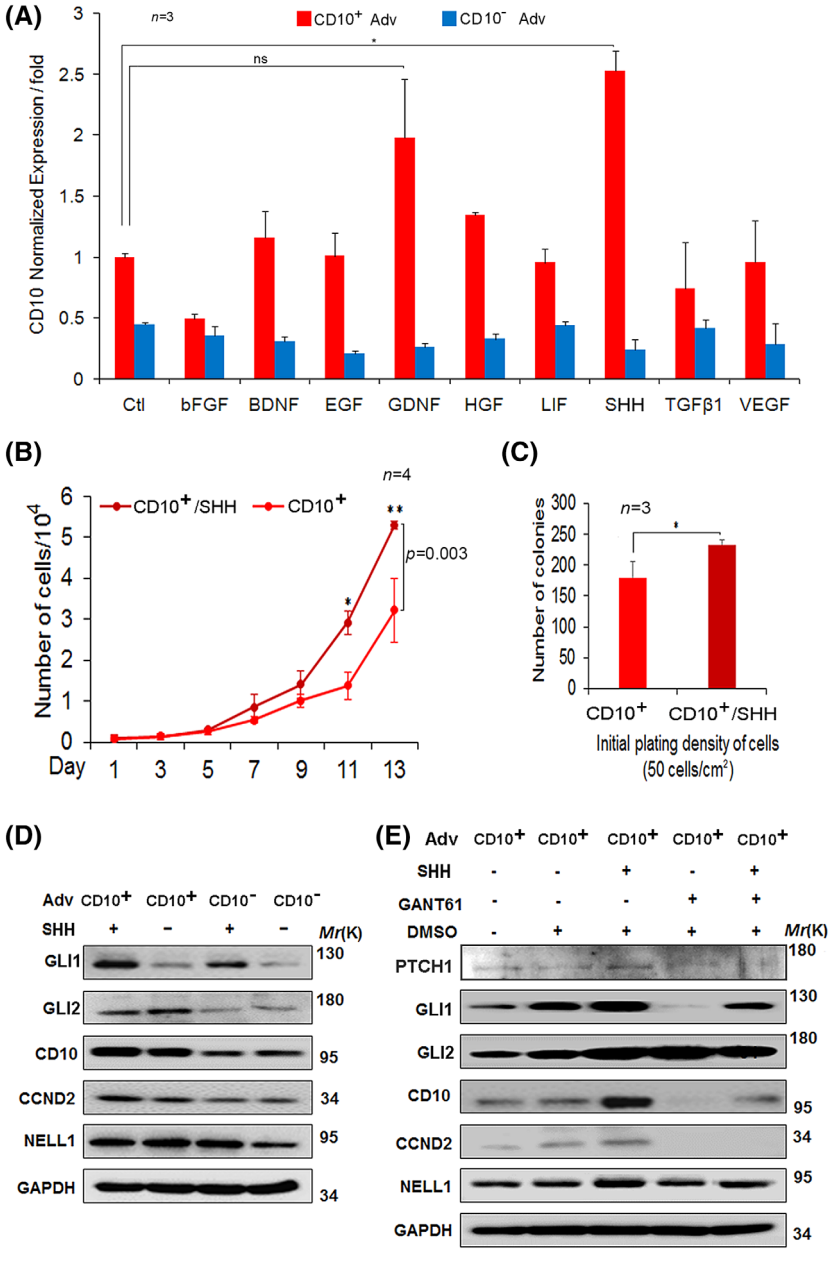

FIGURE 7 SHH/GLI1 induces CD10-related gene expression in WAT CD10$^+$ adventitial cells. A, Among all growth factors used, only SHH (100 ng/mL) induces CD10 expression in CD10$^+$ adventitial cells but not in CD10$^-$ adventitial cells (mean ± SD, n = 3). *$P < .05$; **$P < .01$. One-way analysis of variance (ANOVA) with the Student-Newman-Keuls test. B, CD10$^+$ adventitial cell numbers after SHH induction (100 ng/mL) when seeded at 500 cells/cm^2 (mean ± SD, n = 4). *$P < .05$; **$P < .01$. One-tailed t-test. C, CFU-f content in CD10$^+$ adventitial cells after SHH induction (100 ng/mL) when seeded at 50 cells/cm^2. Data are displayed as mean ± SD, n = 3. $P = .030$. One-tailed t-test. D, Western bot analysis of GLI1, GLI2, CD10, CCND2, and NELL1 expression in CD10$^+$ and CD10$^-$ adventitial cells after Shh stimulation (n = 3). E, GLI1, GLI2, CD10, CCND2, and NELL1 expression in CD10$^+$ adventitial cells after SHH stimulation and pretreatment with GLI1 inhibitor GANT61 (10 μM) (n = 3). See also Figures S6 and S7. Adv, adventitial cells; CFU, colony-forming unit; SHH, sonic hedgehog

3.6 | SHH/GLI1 affects CD10 signaling in CD10$^+$ adventitial cells

CD10 expression increased in CD10$^+$ adventitial cells after treatment with growth factors for 24 hours. In particular, a multisystem morphogen, SHH, could augment CD10 expression over 2.5-fold in CD10$^+$ adventitial cells (Figure 7A). The expression of the multipotency genes *POU5F*, *NANOG*, *SOX2*, and *TERT* was also significantly increased in CD10$^+$ adventitial cells after exposure to SHH ($P < .05$) (Figure S6). Simultaneously, CD10$^+$ adventitial cell proliferation and CFU-f content were significantly increased after stimulation by SHH ($P < .05$) (Figure 7B,C). However, upon osteogenic differentiation, alizarin red and von Kossa staining revealed no significant difference in the bone forming potential of CD10$^+$ adventitial cells stimulated or not by SHH (Figure S7A).

Additionally, protein expression of GLI1, CCND2, and NELL1 was increased after addition of SHH for 48 hours to cultured CD10$^+$ adventitial cells (Figure 7D). When GANT61 was used to block SHH/GLI1 signaling in CD10$^+$ adventitial cells, expression of PTCH1 and GLI1 but also CD10, CCND2, and NELL1 was downregulated (Figure 7E). Even after SHH stimulation for 24 hours of cells pretreated with GANT61, the expression of CD10, CCND2, and NELL1 could not be totally rescued (Figure 7E). In cultured CD10$^-$ adventitial cells, SHH/GLI1 signaling can partly induce CD10 and CCND2 expression (Figure S7B).

4 | DISCUSSION

The *tunica adventitia*, or *tunica externa*, has been the most undervalued layer of the vascular wall, being still often considered as a mere collagen sheath that anchors blood vessels within tissues. Conversely, recent work has identified the adventitia as a niche for progenitor cells involved in tissue turnover and regeneration, as well as fibrotic remodeling.[13,15,17-19,34,38,39] Consistently, adventitial cells in human and mouse organs are a source of MSCs.[17,38] The numerous distinct capabilities of MSCs for multilineage differentiation, immunomodulation, and growth factor and cytokine secretion raise the question of the diversity of these cells and their native forerunners. The heterogeneity of pericytes, another source of MSCs, is being progressively uncovered: pericytes/MSCs expressing the Wnt receptor ROR2 exhibit enhanced chondrogenic potential,[40] whereas a subset of renal juxtaglomerular pericytes as well as their cultured MSC progeny express and produce renin.[41] In the adventitia, a fraction of progenitor cells expressing the GLI1 transcription factor are essential contributors to fibrotic remodeling,[15,38] but the phenotypic and functional diversity of the cells present in this outermost perivascular layer has not been further documented. Here, we show that a subset of adventitial cells expressing the CD10/CALLA cell surface metalloprotease exhibit higher proliferation, clonogenic and osteogenic potentials than their CD10$^-$ counterparts. CD10 expression is upregulated in adventitial cells through SHH/GLI1 signaling. CD10$^+$ adventitial cells increase expression of CCND2 via ERK1/2 and stimulate NELL1 expression via NF-κB. A small subset of cultured CD10-negative adventitial cells was found to express low levels of CD10. This raises the interesting possibility that the low osteogenic potential displayed by cultured CD10$^-$ cells is in fact restricted to this minor culture-induced subset, and that native, tissue resident CD10$^-$ perivascular cells are totally devoid of bone-forming potential.

CD10 is believed to regulate the function of diverse stem cells. Maguer-Satta et al showed that a gradient of peptides generated by CD10 enzyme cleavage is involved, with β1-integrins, in maintaining mammary stem cells and regulating their conversion to luminal progenitors.[33] CD10 expression by stem cells in the bone marrow, adipose tissue, umbilical cord, hair follicle, and endometrium has been reported.[42-46] CD10 has also been described as a cancer stem cell marker and its expression associated with metastasis and poor survival.[47] In the present study, CD10 upregulated CCND2 expression via ERK1/2 and p-ERK1/2, which shortens the G1 phase of the cell cycle and accelerates DNA replication.[48,49] By analogy with embryonic stem cells,[50] CD10/ERK/CCND2 signaling may regulate the self-renewal of adventitial MSC like progenitor cells.

CD10 has been described before at the surface of hBMSCs differentiating toward the osteogenic lineage.[51] In the present study, CD10$^+$ adventitial cells were found to overexpress NELL1 and exhibit superior osteogenic differentiation capacity, compared with CD10$^-$ counterparts. NELL1 is specific of the osteochondral cell lineage and drives osteogenesis in perivascular stem cells and MSC progeny, via RUNX2 phosphorylation, both in culture and in vivo.[52-54]

Our results suggest that SHH/GLI1 signaling regulates CD10 expression in adventitial cells. The CD10 promoter contains three putative non-consensus binding sequences,[55] suggesting that SHH/GLI1 controls the expression of CD10 during transcription. Many cell types can secrete SHH, including perivascular smooth muscle cells,[56] which might control CD10 expression in the adventitia at a short range. Alternatively, studies on the rodent dental pulp have shown that tooth repair by perivascular MSCs is regulated after injury by SHH secreted by nerves of the neurovascular bundle,[19] adding a candidate source of CD10-regulating factors.

As a possible pathologic correlate of our observations, progenitor cells located in the *tunica adventitia* are reportedly involved in arteriosclerosis by supplying the remodeling vessel with calcifying cells.[38,57] In particular, Kramann and colleagues showed that GLI1+ adventitial MSC-like cells generate osteoblasts that drive arterial calcification in chronic kidney disease induced in mice by ischemia.[38,39] Whether the strongly osteogenic CD10$^+$ subset of adventitial progenitor cells is directly and specifically involved in this process and could become a therapy target is an important question under current investigation.

5 | CONCLUSION

In summary, CD10 signaling in perivascular adventitial cells may be essential to *native* MSC self-renewal and multidifferentiation potential maintenance (Figure S8). SHH/GLI1 and CD10 signaling appears as a key regulator in the natural MSC niche.[39]

ACKNOWLEDGMENTS

We thank Dr. Rui Huang for figures organization, Dr. Fiona Rossi for assistance in flow cytometry, Dr. Yue Lin for the help of human tissues collection, Dr. Xiaoqiang Sheng for preparation of manuscript and Dr. Biyun Xu for assistance of statistical analysis. We thank Dr. Ting Wang and Dr. Yanhong Xu for the preparation of human tissue sections. Lijun Ding is supported by grants from National Key Research and Development Program of China (2018YFC1004700), Nature Science Foundation of China (81871128, 81571391) and Nanjing Medical Science Development Project (ZKX16042). Ruotian Li is supported by a grant from Nature Science Foundation of China (81600353). Haixiang Sun is supported by a grant from Jiangsu Province Social Development Project (BE2018602). For this work, Bruno Péault has been supported by grants from the British Heart Foundation, and BIRAX Regenerative Medicine Initiative. Aaron W. James was supported by the NIH/NIAMS (R01 AR070773, K08 AR068316), NIH/NIDCR (R21 DE027922), Department of Defense (W81XWH-18-1-0121, W81XWH-18-1-0336, W81XWH-18-10613), American Cancer Society (Research Scholar Grant, RSG-18-027-01-CSM), the Maryland Stem Cell Research Foundation, and the Musculoskeletal Transplant Foundation. The content is solely the responsibility of the authors and does not necessarily represent the official views of the National Institute of Health or Department of Defense.

CONFLICT OF INTEREST

A.W.J. declared Consultant/Advisory role with Novadip and research funding from MTF Biologics. The remaining authors declared no potential conflicts of interest.

AUTHOR CONTRIBUTIONS

L.D.: conception and design, collection and assembly of data, data analysis and interpretation, manuscript writing, financial support; B.V.: collection and assembly of data, data analysis and interpretation, manuscript revision and final approval of manuscript; N.K.: provision of study material or patients, collection and assembly of data, data analysis and interpretation; J.S., L.X.: collection and assembly of data, data analysis and interpretation; G.Y., R.L.: administrative support, provision of study material or patients; Y.L.: administrative support, collection and assembly of data; A.G.: collection and assembly of data; Z.D., Z.Y: administrative support; Y.H.: financial support, administrative support; W.R.H.: provision of study material or patients; A.J.: provision of study material or patients, conception of experiments, manuscript revision and final approval of manuscript; H.S., B.P.: conception and design, financial support, data analysis and interpretation, manuscript writing, final approval of manuscript.

DATA AVAILABILITY STATEMENT

Microarray data from this study have been deposited in the GEO (NCBI) under the accession number GEO: GSE115557. The data that support the findings of this study are available from the corresponding authors upon reasonable request.

ORCID

Lijun Ding https://orcid.org/0000-0002-6330-7945
Yali Hu https://orcid.org/0000-0001-5475-7840
Haixiang Sun https://orcid.org/0000-0002-1215-1792

REFERENCES

1. Jiang Y, Jahagirdar BN, Reinhardt RL, et al. Pluripotency of mesenchymal stem cells derived from adult marrow. *Nature*. 2002;418:41-49.
2. Zuk PA, Zhu M, Ashjian P, et al. Human adipose tissue is a source of multipotent stem cells. *Mol Biol Cell*. 2002;13:4279-4295.
3. Dellavalle A, Maroli G, Covarello D, et al. Pericytes resident in postnatal skeletal muscle differentiate into muscle fibres and generate satellite cells. *Nat Commun*. 2011;2:499.
4. Covas DT, Panepucci RA, Fontes AM, et al. Multipotent mesenchymal stromal cells obtained from diverse human tissues share functional properties and gene-expression profile with CD146+ perivascular cells and fibroblasts. *Exp Hematol*. 2008;36:642-654.
5. Schwab KE, Gargett CE. Co-expression of two perivascular cell markers isolates mesenchymal stem-like cells from human endometrium. *Hum Reprod*. 2007;22:2903-2911.
6. Mitchell KE, Weiss ML, Mitchell BM, et al. Matrix cells from Wharton's jelly form neurons and glia. *Stem Cells*. 2003;21:50-60.
7. Miura M, Gronthos S, Zhao M, et al. SHED: stem cells from human exfoliated deciduous teeth. *Proc Natl Acad Sci U S A*. 2003;100:5807-5812.
8. Pittenger MF, Mackay AM, Beck SC, et al. Multilineage potential of adult human mesenchymal stem cells. *Science*. 1999;284:143-147.
9. Tolar J, Le Blanc K, Keating A, et al. Concise review: hitting the right spot with mesenchymal stromal cells. *Stem Cells*. 2010;28:1446-1455.
10. Wei X, Yang X, Han ZP, Qu FF, Shao L, Shi YF. Mesenchymal stem cells: a new trend for cell therapy. *Acta Pharmacol Sin*. 2013;34:747-754.
11. Traktuev DO, Merfeld-Clauss S, Li J, et al. A population of multipotent CD34-positive adipose stromal cells share pericyte and mesenchymal surface markers, reside in a periendothelial location, and stabilize endothelial networks. *Circ Res*. 2008;102:77-85.
12. Gökçinar-Yagci B, Özyüncü Ö, Çelebi-Saltik B. Isolation, characterisation and comparative analysis of human umbilical cord vein perivascular cells and cord blood mesenchymal stem cells. *Cell Tissue Bank*. 2016;17:345-352.
13. Campagnolo P, Cesselli D, Al Haj Zen A, et al. Human adult vena saphena contains perivascular progenitor cells endowed with clonogenic and proangiogenic potential. *Circulation*. 2010;121:1735-1745.
14. Méndez-Ferrer S, Michurina TV, Ferraro F, et al. Mesenchymal and haematopoietic stem cells form a unique bone marrow niche. *Nature*. 2010;466:829-834.
15. Kramann R, Schneider RK, DiRocco DP, et al. Perivascular Gli1+ progenitors are key contributors to injury-induced organ fibrosis. *Cell Stem Cell*. 2015;16:51-66.
16. Crisan M, Yap S, Casteilla L, et al. A perivascular origin for mesenchymal stem cells in multiple human organs. *Cell Stem Cell*. 2008;3:301-313.
17. Corselli M, Chen CW, Sun B, Yap S, Rubin JP, Péault B. The tunica adventitia of human arteries and veins as a source of mesenchymal stem cells. *Stem Cells Dev*. 2012;21:1299-1308.
18. Hardy WR, Moldovan NI, Moldovan L, et al. Transcriptional networks in single perivascular cells sorted from human adipose tissue reveal a hierarchy of mesenchymal stem cells. *Stem Cells*. 2017;35:1273-1289.
19. Zhao H, Feng J, Seidel K, et al. Secretion of shh by a neurovascular bundle niche supports mesenchymal stem cell homeostasis in the adult mouse incisor. *Cell Stem Cell*. 2014;14:160-173.
20. Zhao H, Feng J, Ho TV, Grimes W, Urata M, Chai Y. The suture provides a niche for mesenchymal stem cells of craniofacial bones. *Nat Cell Biol*. 2015;17:386-396.

21. Samanta J, Grund EM, Silva HM, Lafaille JJ, Fishell G, Salzer JL. Inhibition of Gli1 mobilizes endogenous neural stem cells for remyelination. *Nature*. 2015;526:448-452.
22. Caligaris-Cappio F, Bergui L, Tesio L, et al. Identification of malignant plasma cell precursors in the bone marrow of multiple myeloma. *J Clin Invest*. 1985;76:1243-1251.
23. Oba J, Nakahara T, Hayashida S, et al. Expression of CD10 predicts tumor progression and unfavorable prognosis in malignant melanoma. *J Am Acad Dermatol*. 2011;65:1152-1160.
24. Schindelin J, Arganda-Carreras I, Frise E, et al. Fiji: an open-source platform for biological image analysis. *Nat Methods*. 2012;9:676-682.
25. Corselli M, Crisan M, Murray IR, et al. Identification of perivascular mesenchymal stromal/stem cells by flow cytometry. *Cytometry A*. 2013;83:714-720.
26. Smyth GK. Linear models and empirical bayes methods for assessing differential expression in microarray experiments. *Stat Appl Genet Mol Biol*. 2004;3:Article 3.
27. Sturn A, Quackenbush J, Trajanoski Z. Genesis: cluster analysis of microarray data. *Bioinformatics*. 2002;18:207-208.
28. Denkovskij J, Rudys R, Bernotiene E, Minderis M, Bagdonas S, Kirdaite G. Cell surface markers and exogenously induced PpIX in synovial mesenchymal stem cells. *Cytometry A*. 2015;87:1001-1011.
29. Bachelard-Cascales E, Chapellier M, Delay E, et al. The CD10 enzyme is a key player to identify and regulate human mammary stem cells. *Stem Cells*. 2010;28:1081-1088.
30. Ong WK, Tan CS, Chan KL, et al. Identification of specific cell-surface markers of adipose-derived stem cells from subcutaneous and visceral fat depots. *Stem Cell Rep*. 2014;2:171-179.
31. Navarro-Guerrero E, Platero-Luengo A, Linares-Clemente P, Cases I, López-Barneo J, Pardal R. Gene expression profiling supports the neural crest origin of adult rodent carotid body stem cells and identifies CD10 as a marker for mesectoderm-committed progenitors. *Stem Cells*. 2016;34:1637-1650.
32. Sidney LE, Branch MJ, Dunphy SE, Dua HS, Hopkinson A. Concise review: evidence for CD34 as a common marker for diverse progenitors. *STEM CELLS*. 2014;32:1380-1389.
33. Maguer-Satta V, Besançon R, Bachelard-Cascales E. Concise review: neutral endopeptidase (CD10): a multifaceted environment actor in stem cells, physiological mechanisms, and cancer. *STEM CELLS*. 2011;29:389-396.
34. Braun J, Kurtz A, Barutcu N, Bodo J, Thiel A, Dong J. Concerted regulation of CD34 and CD105 accompanies mesenchymal stromal cell derivation from human adventitial stromal cell. *Stem Cells Dev*. 2013;22:815-827.
35. O'Malley J, Skylaki S, Iwabuchi KA, et al. High-resolution analysis with novel cell-surface markers identifies routes to iPS cells. *Nature*. 2013;499:88-91.
36. Koyama-Nasu R, Nasu-Nishimura Y, Todo T, et al. The critical role of cyclin D2 in cell cycle progression and tumorigenicity of glioblastoma stem cells. *Oncogene*. 2013;32:3840-3845.
37. Lee S, Zhang X, Shen J, et al. Human perivascular stem cells and Nel-Like protein-1 synergistically enhance spinal fusion in osteoporotic rats. *STEM CELLS*. 2015;33:3158-3163.
38. Kramann R, Goettsch C, Wongboonsin J, et al. Adventitial MSC-like cells are progenitors of vascular smooth muscle cells and drive vascular calcification in chronic kidney disease. *Cell Stem Cell*. 2016;19:628-642.
39. Baker AH, Péault B. A Gli(1)ttering Role for Perivascular Stem Cells in Blood Vessel Remodeling. *Cell Stem Cell*. 2016;19:563-565.
40. Dickinson SC, Sutton CA, Williams RL, et al. The Wnt5a receptor ROR2 is a predictive cell surface marker of human mesenchymal stem cells with an enhanced capacity for chondrogenic differentiation. *STEM CELLS*. 2017;35:2280-2291.
41. Shaw I, Rider S, Mullins J, Hughes J, Péault B. Pericytes in the renal vasculature: roles in health and disease. *Nat Rev Nephrol*. 2018;14:521-534.
42. Rasini V, Dominici M, Kluba T, et al. Mesenchymal stromal/stem cells markers in the human bone marrow. *Cytotherapy*. 2013;15:292-306.
43. Nikoo S, Ebtekar M, Jeddi-Tehrani M, et al. Menstrual blood-derived stromal stem cells from women with and without endometriosis reveal different phenotypic and functional characteristics. *Mol Hum Reprod*. 2014;20:905-918.
44. Farias VA, Linares-Fernández JL, Peñalver JL, et al. Human umbilical cord stromal stem cell express CD10 and exert contractile properties. *Placenta*. 2011;32:86-95.
45. Linnemann JR, Miura H, Meixner LK, et al. Quantification of regenerative potential in primary human mammary epithelial cells. *Development*. 2015;142:3239-3251.
46. Morisaki N, Ohuchi A, Moriwaki S. The role of neprilysin in regulating the hair cycle. *PLoS One*. 2013;8:e55947.
47. Fukusumi T, Ishii H, Konno M, et al. CD10 as a novel marker of therapeutic resistance and cancer stem cells in head and neck squamous cell carcinoma. *Br J Cancer*. 2014;111:506-514.
48. Lee J, Kanatsu-Shinohara M, Morimoto H, et al. Genetic reconstruction of mouse spermatogonial stem cell self-renewal in vitro by Ras-cyclin D2 activation. *Cell Stem Cell*. 2009;5:76-86.
49. Tsunekawa Y, Britto JM, Takahashi M, Polleux F, Tan SS, Osumi N. Cyclin D2 in the basal process of neural progenitors is linked to non-equivalent cell fates. *EMBO J*. 2012;31:1879-1892.
50. Becker KA, Ghule PN, Lian JB, Stein JL, van Wijnen AJ, Stein GS. Cyclin D2 and the CDK substrate p220(NPAT) are required for self-renewal of human embryonic stem cells. *J Cell Physiol*. 2010;222:456-464.
51. Granéli C, Thorfve A, Ruetschi U, et al. Novel markers of osteogenic and adipogenic differentiation of human bone marrow stromal cells identified using a quantitative proteomics approach. *Stem Cell Res*. 2014;12:153-165.
52. Zhang X, Péault B, Chen W, et al. The Nell-1 growth factor stimulates bone formation by purified human perivascular cells. *Tissue Eng Part A*. 2011;17:2497-2509.
53. Pang S, Shen J, Liu Y, et al. Proliferation and osteogenic differentiation of mesenchymal stem cells induced by a short isoform of NELL-1. *STEM CELLS*. 2015;33:904-915.
54. Zhang X, Ting K, Bessette CM. Nell-1, a key functional mediator of Runx2, partially rescues calvarial defects in Runx2(+/−) mice. *J Bone Miner Res*. 2011;26:777-791.
55. Winklmayr M, Schmid C, Laner-Plamberger S, et al. Non-consensus GLI binding sites in Hedgehog target gene regulation. *BMC Mol Biol*. 2010;11:2.
56. Wang G, Zhang Z, Xu Z, et al. Activation of the sonic hedgehog signaling controls human pulmonary arterial smooth muscle cell proliferation in response to hypoxia. *Biochim Biophys Acta*. 2010;1803:1359-1367.
57. Psaltis PJ, Simari RD. Vascular wall progenitor cells in health and disease. *Circ Res*. 2015;116:1392-1412.

SUPPORTING INFORMATION

Additional supporting information may be found online in the Supporting Information section.

How to cite this article: Ding L, Vezzani B, Khan N, et al. CD10 expression identifies a subset of human perivascular progenitor cells with high proliferation and calcification potentials. *Stem Cells*. 2020;38:261–275. https://doi.org/10.1002/stem.3112